Usage of modal synthesis method with condensation in rotor dynamics

V. Zeman[a,*], J. Šašek[a]

[a]*Faculty of Applied Sciences, University of West Bohemia in Pilsen, Univerzitní 22, 306 14 Plzeň, Czech Republic*

Abstract

The paper deals with mathematical modelling of vibration and modal analysis of rotors composed of a flexible shaft and several flexible disks. The shaft is modelled as a one dimensional continuum whereon flexible disks modelled as a three dimensional continuum are rigid mounted to shaft. The presented approach allows to introduce continuously distributed centrifugal and gyroscopic effects. The finite element method was used for shaft and disks discretization. The modelling of such flexible multi-body rotors with large DOF number is based on the system decomposition into subsystems and on the modal synthesis method with condensation. Lower vibration mode shapes of the mutually uncoupled and non-rotating subsystems are used for creation of the rotor condensed mathematical model. An influence of the different level of a rotor condensation model on the accuracy of calculated eigenfrequencies and eigenvectors is discussed.

Keywords: rotor dynamics, modal synthesis method, condensation, eigenvalues, eigenvectors

1. Introduction

Many rotating systems with disks (gears, wheels, rings) are modelled as one-dimensional rotating shafts with rigid disks attached to them [4, 5, 11]. This approach can be usually applied on rotating systems excited in time periodic (harmonic) forces and moments with frequency corresponding to operating speed and its multiple. However, there are systems (high speed gears, bladed disks in turbomachines, engine rotors, wheels of rail vehicles) in which the natural modes of the disks can not be neglected.

Many publications are dedicated to the dynamic analysis of thin rotating disks. One of newest and most comprehensive publication is the monograph of Genta [2]. Started from the classical membrane theory for thin disks there are shown some possible approaches for modelling general three dimensional rotors and disks considering gyroscopic and centrifugal effects. In all to us know publications the flexible disk is modelled separately as an isolated subsystem or as a flexible disk linked on the internal or external surfaces to rigid body rotating with constant angular velocity. The rigid and flexible coupling between disk and the shaft was modelled in author's publications [3, 8] dealing with a special test rotor with one disk.

The main aim of this article is to present a generally accepted modal synthesis method with reduction DOF number (so-called condensation) for modelling of flexible multi-body rotor vibrations. This method is applied on rotors composed of a flexible shaft and several flexible disks discretized in a rotating coordinate system using FE method. Rigid constraints between disks and outer shaft surfaces are under consideration.

---

*Corresponding author. Tel.: +420 377 632 332, e-mail: zemanv@kme.zcu.cz.

2. Mathematical model of the shaft with several disks

We suppose that only small deformations occur in the elastic bodies, so that the overall body motion can be described by large rotation of a rotor reference frame xyz superimposed by small linear deformations given by some elastic coordinates.

We will decompose the rotating shaft with disks (Fig. 1) into subsystems — disk subsystems (subscript $s = 1, 2, \ldots$) and a shaft subsystem (subscript S). It is supposed that the reference frame rotates with constant operational angular velocity ω around its X-axis.

According to the derivation in the book [6] the disks can be discretized in the rotating xyz-coordinate system using linear isoparametric hexahedral finite elements (Fig. 2). The equations of motion for deformable disks can be written in a configuration space defined by the vector

$$\boldsymbol{q}_s = [\ldots u_j\, v_j\, w_j \ldots]^T \in \boldsymbol{R}^{n_s},\ s = 1, 2, \ldots \tag{1}$$

of nodal j displacements in x, y, z-directions (see Fig. 1). The superscripts corresponding to free (F) or coupled (C) node elastic coordinates of the disks in the expression (1) are not meanwhile reflected. The motion equations of undamped and uncoupled rotating disks were derived in [10] using Lagrange equations in the form

$$\boldsymbol{M}_s \ddot{\boldsymbol{q}}_s(t) + \omega \boldsymbol{G}_s \dot{\boldsymbol{q}}_s(t) + (\boldsymbol{K}_s - \omega^2 \boldsymbol{K}_{\omega,s})\boldsymbol{q}_s(t) = \omega^2 \boldsymbol{f}_s,\ s = 1, 2, \ldots \tag{2}$$
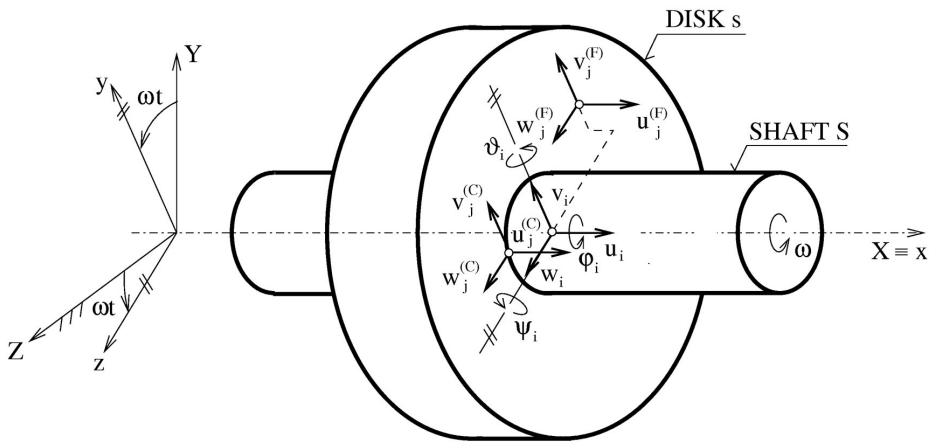

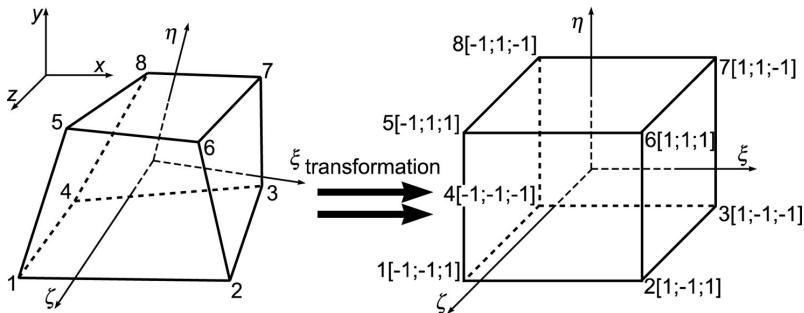Fig. 1. Scheme of the shaft and the disk coordinate system

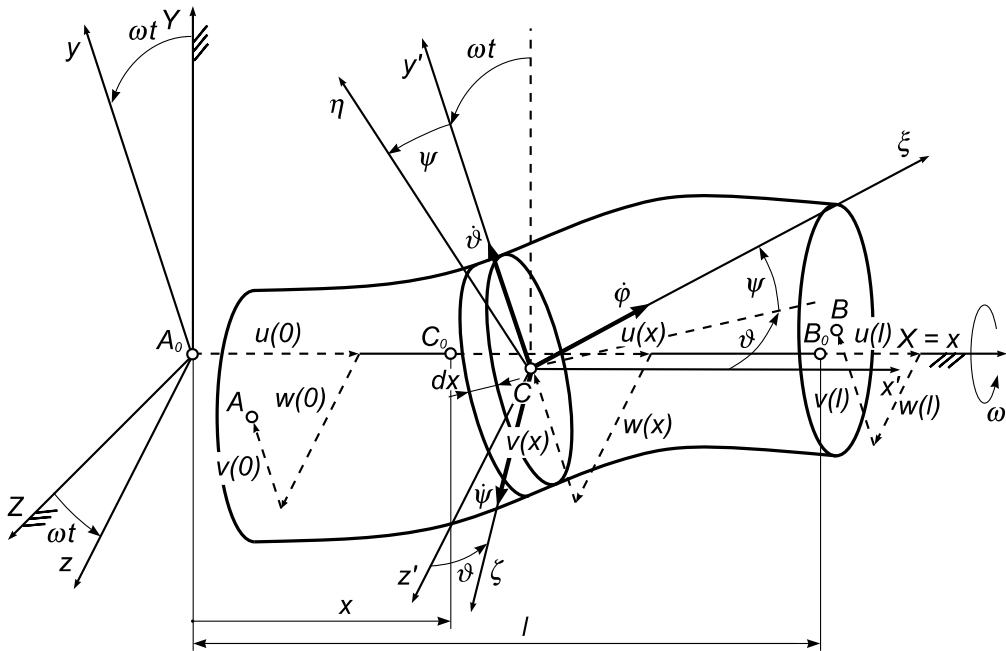Fig. 2. Scheme of the linear isoparametric hexahedral element

Fig. 3. Scheme of the shaft finite element

where mass $\boldsymbol{M}_s$, static stiffness $\boldsymbol{K}_s$ and dynamic stiffness $\boldsymbol{K}_{\omega,s}$ matrices are symmetric and skew-symmetric matrices $\omega\boldsymbol{G}_s$ express gyroscopic effects. Centrifugal load vectors $\omega^2\boldsymbol{f}_s$ are constant in time.

The shaft is modelled as an one dimensional continuum on assumption of the undeformable cross-section that is still perpendicular to the shaft centre-line. The shaft is discretized using shaft finite elements [7] with two nodes A, B (see Fig. 3). The derivation of the motion equations is in [7] shown in non-rotating coordinate system XYZ. To our purpose the mathematical model must be derived in rotating coordinate system xyz — [9] as for disks. The elastic displacements of each node i on the shaft centre-line are described by six generalized coordinates — three displacements u_i, v_i, w_i in x, y, z — directions and three rotation angles φ_i, ϑ_i, ψ_i (see Fig. 1). The bending displacements $v(x,t)$, $w(x,t)$ of the arbitrary shaft finite element point C_0 on the shaft centre-line at the position x from nodal point A_0 (see Fig. 3) are approximated by cubic polynomials of variable x, longitudinal $u(x,t)$ and torsion $\varphi_i(x,t)$ displacements are approximated by linear polynomials. Supposed small Eulerian angles satisfy the conditions

$$\vartheta(x,t) = -\frac{\partial w(x,t)}{\partial x}, \ \psi(x,t) = \frac{\partial v(x,t)}{\partial x}. \tag{3}$$

The motion equations of the shaft can be written in configuration space defined by vector

$$\boldsymbol{q}_S = [\ldots u_i\, v_i\, w_i\, \varphi_i\, \vartheta_i\, \psi_i \ldots]^T \in \boldsymbol{R}^{n_S} \tag{4}$$

of nodal i displacements (see Fig. 1). The conservative mathematical model of the rotating uncoupled shaft supported on rolling-element bearings has the form [9]

$$\boldsymbol{M}_S\ddot{\boldsymbol{q}}_S(t) + \omega\boldsymbol{G}_S\dot{\boldsymbol{q}}_S(t) + (\boldsymbol{K}_S - \omega^2\boldsymbol{K}_{\omega,S} + \boldsymbol{K}_B(t))\boldsymbol{q}_s(t) = \boldsymbol{0}, \tag{5}$$

where mass $\boldsymbol{M}_S$, static stiffness $\boldsymbol{K}_S$ and dynamic stiffness $\boldsymbol{K}_{\omega,S}$ matrices are symmetric and gyroscopic matrix $\omega \boldsymbol{G}_S$ is skew-symmetric. The linearized rolling-element bearings are generally described by in time harmonic varying symmetric stiffness matrix

$$\boldsymbol{K}_B(t) = \boldsymbol{K}_B + \Delta\boldsymbol{K}_C \cos(2\omega t) + \Delta\boldsymbol{K}_S \sin(2\omega t) \tag{6}$$

where the matrices $\Delta\boldsymbol{K}_C$ and $\Delta\boldsymbol{K}_S$ depend on difference of bearing stiffnesses in two principal axis of stresses. For the isotropic bearings the bearing stiffness matrix is time independent.

The vectors of disk generalized coordinates can be partitioned with respect to the couplings between disks and shaft in the form

$$\boldsymbol{q}_s = \left[\begin{array}{c} \boldsymbol{q}_s^{(F)} \\ \boldsymbol{q}_s^{(C)} \end{array} \right], \; \boldsymbol{q}_s^{(F)} \in \boldsymbol{R}^{n_s^{(F)}}, \; \boldsymbol{q}_s^{(C)} \in \boldsymbol{R}^{n_s^{(C)}}, \; s = 1, 2, \ldots \tag{7}$$

where the displacements of the contact disk nodes on the disk inner surface (shaft outer surface) can be expressed by the displacements of shaft nodes i at its axis in the same ($x_j = x_i$) or near ($x_j \neq x_i$) perpendicular plane (see Fig. 1). This relation for displacements of nodes j and i is

$$\left[\begin{array}{c} u_j^{(C)} \\ v_j^{(C)} \\ w_j^{(C)} \end{array} \right] = \left[\begin{array}{ccc|ccc} 1 & 0 & 0 & 0 & z_j & -y_j \\ 0 & 1 & 0 & -z_j & 0 & x_j - x_i \\ 0 & 0 & 1 & y_j & -x_j + x_i & 0 \end{array} \right] \left[\begin{array}{c} u_i \\ v_i \\ w_i \\ \varphi_i \\ \vartheta_i \\ \psi_i \end{array} \right] \tag{8}$$

or shortly

$$\boldsymbol{q}_j^{(C)} = \boldsymbol{T}_{j,i} \boldsymbol{q}_i. \tag{9}$$

The displacements of the free (uncoupled) disk nodes are localized in vector $\boldsymbol{q}_s^{(F)} \in \boldsymbol{R}^{n_s^{(F)}}$. The total transformation between displacements of coupled nodes of the disk s with a shaft outer surface can be expressed in the matrix form

$$\left[\begin{array}{c} \vdots \\ \hline \boldsymbol{q}_j^{(C)} \\ \hline \vdots \end{array} \right] = \left[\begin{array}{c|c|c} & \vdots & \\ \hline \cdots & \boldsymbol{T}_{j,i} & \cdots \\ \hline & \vdots & \end{array} \right] \left[\begin{array}{c} \vdots \\ \hline \boldsymbol{q}_i \\ \hline \vdots \end{array} \right] \Longrightarrow \boldsymbol{q}_s^{(C)} = \boldsymbol{T}_{s,S} \boldsymbol{q}_S \tag{10}$$

where the transformation rectangular matrix is $\boldsymbol{T}_{s,S} \in \boldsymbol{R}^{n_s^{(C)}, n_S}$ and $n_s^{(C)} = n_s - n_s^{(F)}$ is DOF number corresponding to coupled nodes of the disk s.

3. Condensed mathematical model of the rotor

The nodal coordinates of the disk finite element models can be used directly as elastic coordinates, although the number of degrees of freedom required to adequately represent the deformation may be very large. Hence, the number of free node elastic coordinates $\boldsymbol{q}_s^{(F)}$ of the disks is desirable to reduce by the use of modal condensation [7]. For that purpose each matrix and vector in the disk mathematical models (2) can be rearranged according to decomposition (7)

$$\boldsymbol{X}_s = \left[\begin{array}{cc} \boldsymbol{X}_s^{FF} & \boldsymbol{X}_s^{FC} \\ \boldsymbol{X}_s^{CF} & \boldsymbol{X}_s^{CC} \end{array} \right], \boldsymbol{X} = \boldsymbol{M}, \, \boldsymbol{G}, \, \boldsymbol{K}, \, \boldsymbol{K}_\omega, \, \boldsymbol{f}_s = \left[\begin{array}{c} \boldsymbol{f}_s^{(F)} \\ \boldsymbol{f}_s^{(C)} \end{array} \right], \, s = 1, 2, \ldots \tag{11}$$

Let modal properties of the conservative model of the isolated non-rotating disk s (for $\omega = 0$) be characterized by spectral and modal matrices satisfying the orthogonality conditions

$$\boldsymbol{V}_s^T \boldsymbol{M}_s \boldsymbol{V}_s = \boldsymbol{E}, \ \boldsymbol{V}_s^T \boldsymbol{K}_s \boldsymbol{V}_s = \boldsymbol{\Lambda}_s, \ s = 1, 2, \ldots \tag{12}$$

where $\boldsymbol{E}$ is unit matrix. Modal matrices of disks can be rearranged into the block form

$$\boldsymbol{V}_s = \left[\begin{array}{cc} {}^m\boldsymbol{V}_s^F & {}^s\boldsymbol{V}_s^F \\ {}^m\boldsymbol{V}_s^C & {}^s\boldsymbol{V}_s^C \end{array} \right], \ s = 1, 2, \ldots \tag{13}$$

corresponding to decomposition (7) and eigenvectors are separated into frequency lower eigenvectors (so called master — superscript m) and frequency higher eigenvectors (so called slave — superscript s).The vectors $\boldsymbol{q}_s^{(F)}$, corresponding to free disk nodes, can be approximately transformed in the form

$$\boldsymbol{q}_s^{(F)} = {}^m\boldsymbol{V}_s^F \boldsymbol{x}_s, \ s = 1, 2, \ldots, \tag{14}$$

where ${}^m\boldsymbol{V}_s^F \in \boldsymbol{R}^{n_s^{(F)}, m_s^{(F)}}$ is the modal submatrix of the disk s corresponding to free disk generalized coordinates and frequency lower eigenmodes. Higher natural modes usually contribute less to the disk deformation and their influence can be neglected.

The motion equations of the fictive undamped system assembled from uncoupled subsystems — the shaft supported by bearings and isolated disks — in the configuration space

$$\boldsymbol{q} = \left[(\boldsymbol{q}_1^{(F)})^T \ (\boldsymbol{q}_1^{(C)})^T \ (\boldsymbol{q}_2^{(F)})^T \ (\boldsymbol{q}_2^{(C)})^T \ \ldots \boldsymbol{q}_S^T \right]^T \tag{15}$$

can be formally rewritten as

$$\boldsymbol{M}\ddot{\boldsymbol{q}}(t) + \omega \boldsymbol{G}\dot{\boldsymbol{q}}(t) + (\boldsymbol{K} - \omega^2 \boldsymbol{K}_\omega)\boldsymbol{q}(t) = \omega^2 \boldsymbol{f} \tag{16}$$

where, according to mathematical models (2) and (5), matrices have the block-diagonal form $\boldsymbol{X} = \text{diag}(\boldsymbol{X}_1, \boldsymbol{X}_2, \ldots, \boldsymbol{X}_S)$, $\boldsymbol{X} = \boldsymbol{M}, \boldsymbol{G}, \boldsymbol{K}_\omega$ and $\boldsymbol{K} = \text{diag}(\boldsymbol{K}_1, \boldsymbol{K}_2, \ldots, \boldsymbol{K}_S + \boldsymbol{K}_B(t))$, and $\boldsymbol{f} = [\boldsymbol{f}_1, \boldsymbol{f}_2, \ldots, \boldsymbol{0}]^T$. The vector of generalized coordinates $\boldsymbol{q}$ in consequence of the couplings (10), modal transformations (14) and $\boldsymbol{q}_S = \boldsymbol{V}_S \boldsymbol{x}_S$ can be transformed into new vector $\boldsymbol{x} = [\boldsymbol{x}_1, \boldsymbol{x}_2, \ldots, \boldsymbol{x}_S]^T$ of the dimension $m = \sum_s m_s^{(F)} + n_S$. The transformation is given by

$$\left[\begin{array}{c} \boldsymbol{q}_1^{(F)} \\ \boldsymbol{q}_1^{(C)} \\ \boldsymbol{q}_2^{(F)} \\ \boldsymbol{q}_2^{(C)} \\ \hline \vdots \\ \hline \boldsymbol{q}_S \end{array} \right] = \left[\begin{array}{cccc|c} {}^m\boldsymbol{V}_1^F & & & & \cdots \\ & & & & \cdots \\ & & {}^m\boldsymbol{V}_2^F & & \cdots \\ & & & & \cdots \\ \hline \vdots & \vdots & & \ddots & \vdots \\ & & & & \cdots \end{array} \begin{array}{|c} \cdots \\ \boldsymbol{T}_{1,S}\boldsymbol{V}_S \\ \cdots \\ \boldsymbol{T}_{2,S}\boldsymbol{V}_S \\ \hline \vdots \\ \boldsymbol{V}_S \end{array} \right] \left[\begin{array}{c} \boldsymbol{x}_1 \\ \boldsymbol{x}_2 \\ \hline \vdots \\ \hline \boldsymbol{x}_S \end{array} \right] \text{ or shortly } \boldsymbol{q} = \tilde{\boldsymbol{T}} \boldsymbol{x}. \tag{17}$$

The matrix $\boldsymbol{V}_S$ is the full modal matrix of the shaft supported by isotropic bearings ($\Delta \boldsymbol{K}_C = \Delta \boldsymbol{K}_S = \boldsymbol{0}$), satisfying the conditions $\boldsymbol{V}_S^T \boldsymbol{M}_S \boldsymbol{V}_S = \boldsymbol{E}$, and $\boldsymbol{V}_S^T (\boldsymbol{K}_S + \boldsymbol{K}_B)\boldsymbol{V}_S = \boldsymbol{\Lambda}_S$.

The condensed mathematical model of the rotor in the configuration space $\boldsymbol{x}$ takes the form

$$\tilde{\boldsymbol{M}}\ddot{\boldsymbol{x}}(t) + \omega \tilde{\boldsymbol{G}}\dot{\boldsymbol{x}}(t) + (\tilde{\boldsymbol{K}} - \omega^2 \tilde{\boldsymbol{K}}_\omega)\boldsymbol{x}(t) = \omega^2 \tilde{\boldsymbol{f}}, \tag{18}$$

where condensed mass, gyroscopic, static stiffness and dynamic stiffness matrices are given by $\tilde{\boldsymbol{X}} = \tilde{\boldsymbol{T}}^T \boldsymbol{X} \tilde{\boldsymbol{T}}$, $\boldsymbol{X} = \boldsymbol{M}, \boldsymbol{G}, \boldsymbol{K}, \boldsymbol{K}_\omega$, and $\tilde{\boldsymbol{f}} = \tilde{\boldsymbol{T}}^T \boldsymbol{f}$. The transformated matrices of the condensed model (18) for $\boldsymbol{X} = \boldsymbol{M}, \boldsymbol{G}, \boldsymbol{K}, \boldsymbol{K}_\omega$ have the block form

$$
\tilde{\boldsymbol{X}} = \left[\begin{array}{ccc|c}
(^m\boldsymbol{V}_1^F)^T \boldsymbol{X}_1^{FFm} \boldsymbol{V}_1^F & \boldsymbol{0} & \cdots & (^m\boldsymbol{V}_1^F)^T \boldsymbol{X}_1^{FC} \boldsymbol{T}_{1,S} \boldsymbol{V}_S \\
\boldsymbol{0} & (^m\boldsymbol{V}_2^F)^T \boldsymbol{X}_2^{FFm} \boldsymbol{V}_2^F & \cdots & (^m\boldsymbol{V}_2^F)^T \boldsymbol{X}_2^{FC} \boldsymbol{T}_{2,S} \boldsymbol{V}_S \\
\hline
\vdots & \vdots & \ddots & \vdots \\
\hline
\boldsymbol{V}_S^T \boldsymbol{T}_{1,S}^T \boldsymbol{X}_1^{CFm} \boldsymbol{V}_1^F & \boldsymbol{V}_S^T \boldsymbol{T}_{2,S}^T \boldsymbol{X}_2^{CFm} \boldsymbol{V}_2^F & \cdots & \sum_s \boldsymbol{V}_S^T \boldsymbol{T}_{s,S}^T \boldsymbol{X}_s^{CC} \boldsymbol{T}_{s,S} \boldsymbol{V}_s + \boldsymbol{V}_S^T \boldsymbol{X}_S \boldsymbol{V}_S
\end{array} \right]
$$
(19)

and transformed vector of centrifugal load is

$$
\tilde{\boldsymbol{f}} = \left[\begin{array}{c}
(^m\boldsymbol{V}_1^F)^T \boldsymbol{f}_1^{(F)} \\
(^m\boldsymbol{V}_2^F)^T \boldsymbol{f}_2^{(F)} \\
\hline
\vdots \\
\hline
\sum_s \boldsymbol{V}_S^T \boldsymbol{T}_{s,S}^T \boldsymbol{f}_s^{(C)}
\end{array} \right]
$$
(20)

4. Application

Presented method is tested on a simple test example of a steel rotor, which is supported on two isotropic rolling-element bearings. The rotor is consisted of two disks and a shaft (see Fig. 4). The left disk is placed between the bearings and is discretized by 576 finite elements (2 520 DOF). The number of 120 disk nodes is conected to 5 shaft nodes (-360 DOF). The right disk is cantilevered behind the bearing and is discretized by 360 finite elements (1 728 DOF). The number of 96 disk nodes is jointed to 4 shaft nodes (-288 DOF). The shaft is modelled by the 22 shaft finite elements (138 DOF). The condensed model of the whole system was assembled in MATLAB code on the basis of the presented methodology.

In the following table the three condensation levels of non-rotating structure are compared for the 20 lowest eigenfrequencies. In the first column the eigenfrequencies of the non-condensed (reference) model with 3 738 DOF number are placed. The other columns correspond to condensed models with using $c = 50$, 100, and 200 DOF number corresponding to the lowest eigenmodes of each isolated disk (238, 338, 538 DOF number of condensed rotor model).

The first eigenfrequency is zero because the rotor can rotate freely as a rigid body around its axis X. The bending eigenmodes are characterized by double eigenfrequencies. A small difference is made by discretization of the disks. The eigenfrequencies in the second column of Tab. 1 correspond to full finite element model (FEM) after the transformation (10). This full model of the rotor results from equation (16) using the transformation

$$
\left[\begin{array}{c}
\boldsymbol{q}_1^{(F)} \\
\boldsymbol{q}_1^{(C)} \\
\boldsymbol{q}_2^{(F)} \\
\boldsymbol{q}_2^{(C)} \\
\hline
\vdots \\
\hline
\boldsymbol{q}_S
\end{array} \right]
=
\left[\begin{array}{cccc|c}
\boldsymbol{E} & & & \cdots & \\
& & & \cdots & \boldsymbol{T}_{1,S} \\
& & \boldsymbol{E} & \cdots & \\
& & & \cdots & \boldsymbol{T}_{2,S} \\
\hline
\vdots & \vdots & \ddots & & \vdots \\
\hline
& & & \cdots & \boldsymbol{E}
\end{array} \right]
\left[\begin{array}{c}
\boldsymbol{q}_1^{(F)} \\
\boldsymbol{q}_2^{(F)} \\
\hline
\vdots \\
\hline
\boldsymbol{q}_S
\end{array} \right]
\text{ or shortly } \boldsymbol{q} = \tilde{\tilde{\boldsymbol{T}}} \boldsymbol{y}.
$$
(21)

According to (17) the transformation matrix originates from $\tilde{\boldsymbol{T}}$ by change the modal submatrices $^m\boldsymbol{V}_s^F$ of the all disks ($s = 1, 2, \ldots$) and the shaft modal matrix $\boldsymbol{V}_S$ for the unit matrix $\boldsymbol{E}$. The

Table 1. Comparison of rotor eigenfrequencies with different condensation level of disks

eig. mod.	full model	condensed models (condensation level c)					
		$c = 50$		$c = 100$		$c = 200$	
i	f_i [Hz]	f_i [Hz]	ε [%]	f_i [Hz]	ε [%]	f_i [Hz]	ε [%]
1	0.00	0.00	0.00	0.00	0.00	0.00	0.00
2	403.00	404.94	0.48	404.67	0.42	403.78	0.19
3	403.37	405.30	0.48	405.04	0.41	404.14	0.19
4	683.47	685.66	0.32	684.39	0.13	683.92	0.06
5	893.17	894.87	0.19	894.12	0.11	893.61	0.05
6	919.80	925.97	0.67	924.99	0.56	922.24	0.27
7	919.86	926.02	0.67	925.03	0.56	922.29	0.26
8	1 540.55	1 571.24	1.99	1 566.25	1.67	1 551.44	0.71
9	1 542.29	1 572.33	1.95	1 567.40	1.63	1 552.87	0.69
10	2 549.02	2 586.36	1.46	2 583.98	1.37	2 563.15	0.55
11	2 549.35	2 617.48	2.67	2 584.12	1.36	2 563.38	0.55
12	2 879.60	2 891.33	0.41	2 885.87	0.22	2 883.14	0.12
13	3 238.07	3 238.07	0.00	3 238.07	0.00	3 238.07	0.00
14	3 249.22	3 249.22	0.00	3 249.22	0.00	3 249.22	0.00
15	6 092.97	6 111.39	0.30	6 105.31	0.20	6 098.43	0.09
16	6 515.84	6 555.02	0.60	6 532.84	0.26	6 525.35	0.15
17	6 587.20	6 587.21	0.00	6 587.21	0.00	6 587.20	0.00
18	6 634.50	6 634.51	0.00	6 634.51	0.00	6 634.50	0.00
19	6 711.18	6 803.46	1.38	6 793.64	1.23	6 745.76	0.52
20	6 711.19	6 867.36	2.33	6 793.64	1.23	6 745.77	0.52

mathematical model of the rotor in the configuration space y takes the form

$$\tilde{\tilde{M}}\ddot{y}(t) + \omega\tilde{\tilde{G}}\dot{y}(t) + (\tilde{\tilde{K}} - \omega^2\tilde{\tilde{K}}_\omega)y(t) = \omega^2\tilde{\tilde{f}}, \tag{22}$$

where $\tilde{\tilde{X}} = \tilde{\tilde{T}}^T X \tilde{\tilde{T}}$, $X = M, G, K, K_\omega$, and $\tilde{\tilde{f}} = \tilde{\tilde{T}}^T f$.
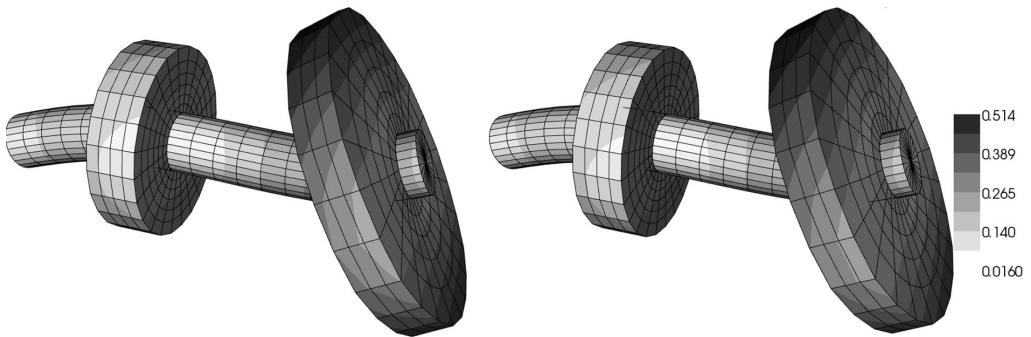

Fig. 4. Comparison of the chosen 8th eigenmode of the referential and condensed model of the rotor

The each eigenfrequency of condensed models is characterized by relative error ε. Relative errors decrease with decreasing condensation level (DOF number c increases), but the highest condensation level is sufficient because the relative errors are below 3 %. The chosen eigenmode calculated on the referential and condensed model (for $c = 50$) is compared in Fig. 4. The referential eigenmode is on the left side and the corresponding eigenmode of the condensed model with 50 DOF number for each disk is on the right side.

4.1. Comparison of modal properties of condensed models with the full FEM of the rotor

Modal properties — eigenfrequencies and eigenvectors for $\omega = 0$ — are a suitable criterion for comparison the full FEM with condensed models of rotors. Eigenfrequencies are usually compared by the relative cumulative error

$$\varepsilon_{50} = \sum_{\nu=2}^{50} \frac{|f_\nu(m_1^{(F)}, m_2^{(F)}, \ldots) - f_\nu|}{f_\nu} \tag{23}$$

where $f_\nu(m_1^{(F)}, m_2^{(F)}, \ldots)$ are eigenfrequencies of the condensed model with reduced degrees of freedom (DOFs) of free node elastic coordinates $q_s^{(F)}$ of the disks and f_ν are pairing frequencies of the full FEM of the rotor. The relative cumulative error of the test rotor (Fig. 4) is shown in Fig. 5 in dependence on numbers of master eigenvectors $m_1^{(F)}$ and $m_2^{(F)}$ of the disks. Fig. 6 shows the maximal relative error

$$\varepsilon_{max} = \max_\nu \frac{|f_\nu(m_1^{(F)}, m_2^{(F)}, \ldots) - f_\nu|}{f_\nu}, \ \nu = 2, 3, \ldots, 50. \tag{24}$$

The modal assurance criterion (MAC) is the suitable tool for the qualitative comparison of eigenvectors. A modified MAC, weighted by the mass matrix, is defined according to [1] as

$$MAC_{ij} = \frac{|\boldsymbol{q}_i^T(m_1^{(F)}, m_2^{(F)}, \ldots)\boldsymbol{M}\boldsymbol{q}_j|}{\left[\boldsymbol{q}_i^T(m_1^{(F)}, m_2^{(F)}, \ldots)\boldsymbol{M}\boldsymbol{q}_i(m_1^{(F)}, m_2^{(F)}, \ldots)\right]\left[\boldsymbol{q}_j^T \boldsymbol{M}\boldsymbol{q}_j\right]} \tag{25}$$
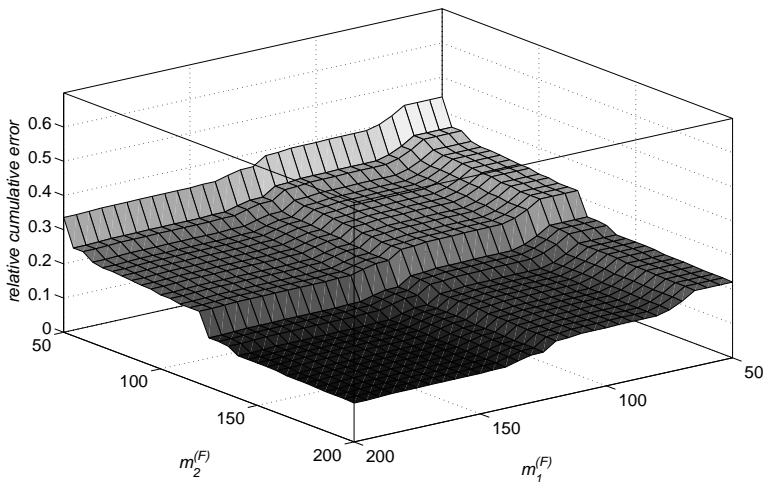

Fig. 5. Relative cumulative error of test rotor eigenfrequencies (for $\nu = 2, 3, \ldots, 50$)
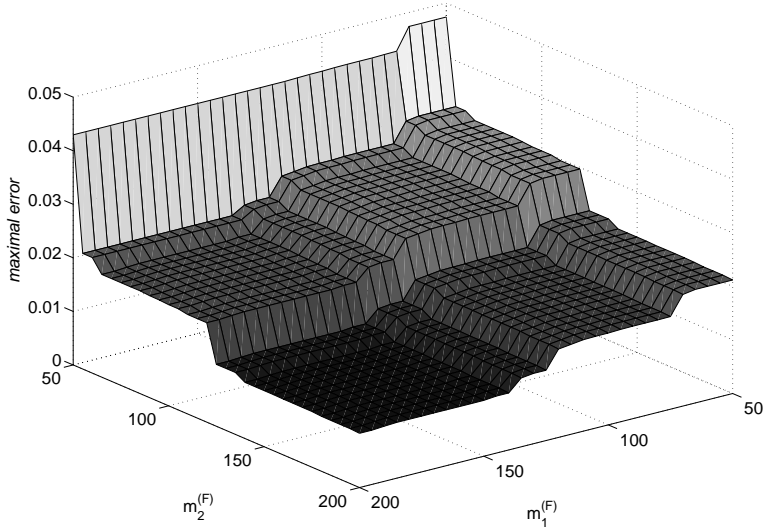
Fig. 6. Maximal relative error of a single eigenfrequency from the eigenfrequency set for $\nu = 2, 3, \ldots, 50$
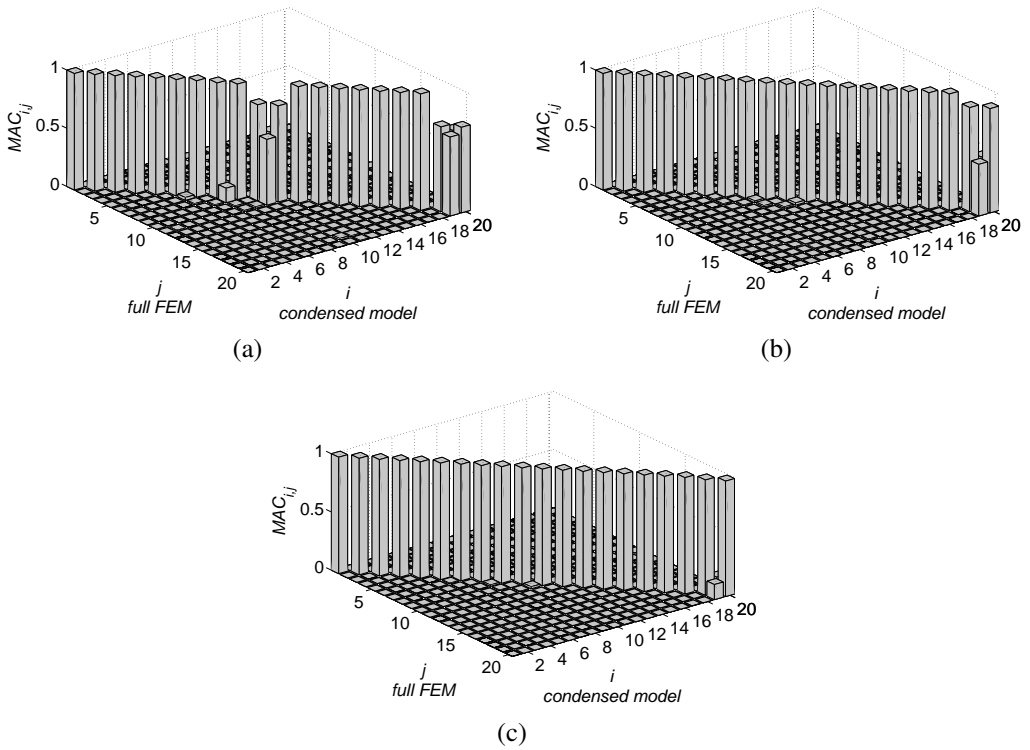

Fig. 7. $\boldsymbol{MAC}$ matrix of the first twenty correlated mode pairs of the test rotor: (a) $m_1^{(F)} = m_2^{(F)} = 50$; (b) $m_1^{(F)} = m_2^{(F)} = 100$; (c) $m_1^{(F)} = m_2^{(F)} = 200$

where $\boldsymbol{q}_i(m_1^{(F)}, m_2^{(F)}, \ldots)$ are eigenvectors of the condensed model and $\boldsymbol{q}_j$ are eigenvectors of the full FEM of the rotor, whereas $\boldsymbol{q}_i(m_1^{(F)}, m_2^{(F)}, \ldots)$ and $\boldsymbol{q}_i$, $\boldsymbol{q}_j(m_1^{(F)}, m_2^{(F)}, \ldots)$ and $\boldsymbol{q}_j$ are pairing eigenvectors.

Using transformations (17) and (21) the MAC can be rewritten in the form of MAC matrix elements

$$MAC_{ij} = \frac{\boldsymbol{x}_i^T \tilde{\boldsymbol{T}}^T \boldsymbol{M} \tilde{\tilde{\boldsymbol{T}}} \boldsymbol{y}_j}{\left[\boldsymbol{x}_i^T \tilde{\boldsymbol{M}} \boldsymbol{x}_i\right] \left[\boldsymbol{y}_j^T \tilde{\tilde{\boldsymbol{M}}} \boldsymbol{y}_j\right]} = \boldsymbol{x}_i^T \tilde{\boldsymbol{T}}^T \boldsymbol{M} \tilde{\tilde{\boldsymbol{T}}} \boldsymbol{y}_j \tag{26}$$

where $\boldsymbol{x}_i$ are eigenvectors of the condensed model (18) and $\boldsymbol{y}_j$ are eigenvectors of the full FEM (22) for $\omega = 0$.

The $\boldsymbol{MAC}$ matrix for the test rotor (Fig. 4) from two sets of individual eigenvectors $\boldsymbol{x_i}$, $\boldsymbol{y_i}$ for $i, j = 1, 2, \ldots, 20$ is shown in Fig. 7 for a different level of a rotor condensation ($m_1^{(F)} = m_2^{(F)} = 50; 100; 200$).

Modal properties of the rotor with angular velocity ω are investigated at the first-order motion equations of the condensed model

$$\begin{bmatrix} \boldsymbol{0} & \tilde{\boldsymbol{M}} \\ \tilde{\boldsymbol{M}} & \omega \tilde{\boldsymbol{G}} \end{bmatrix} \begin{bmatrix} \ddot{\boldsymbol{x}} \\ \dot{\boldsymbol{x}} \end{bmatrix} + \begin{bmatrix} -\tilde{\boldsymbol{M}} & \boldsymbol{0} \\ \boldsymbol{0} & \tilde{\boldsymbol{K}} - \omega^2 \tilde{\boldsymbol{K}}_\omega \end{bmatrix} \begin{bmatrix} \dot{\boldsymbol{x}} \\ \boldsymbol{x} \end{bmatrix} = \boldsymbol{0} \tag{27}$$

corresponding to (18). The eigenvalues $\lambda_\nu = \pm i\Omega_\nu$ are calculated by using mathematical model
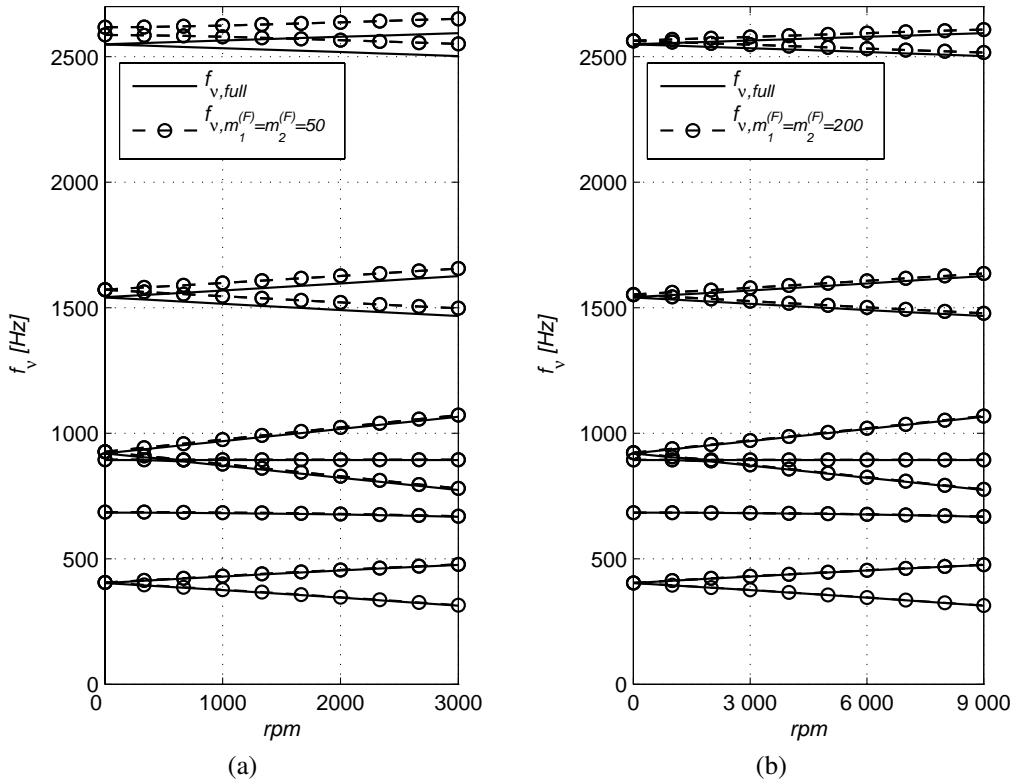

Fig. 8. Campbell diagrams of the test rotor: (a) $m_1^{(F)} = m_2^{(F)} = 50$; (b) $m_1^{(F)} = m_2^{(F)} = 200$

in the form

$$(\boldsymbol{A} - \lambda \boldsymbol{E})\boldsymbol{u} = \boldsymbol{0}, \tag{28}$$

where

$$\boldsymbol{A} = \begin{bmatrix} -\omega \tilde{\boldsymbol{M}}^{-1} \tilde{\boldsymbol{G}} & -\tilde{\boldsymbol{M}}^{-1}(\tilde{\boldsymbol{K}} - \omega^2 \tilde{\boldsymbol{K}}_\omega) \\ \boldsymbol{E} & \boldsymbol{0} \end{bmatrix}, \ \boldsymbol{u} = \begin{bmatrix} \dot{\boldsymbol{x}} \\ \boldsymbol{x} \end{bmatrix}. \tag{29}$$

The Campbell diagrams — plots of eigenfrequencies Ω_ν rad/s or $f_\nu = \Omega_\nu/2\pi$ Hz as a function of rotor revolutions per minute $n = 30\omega/\pi$ rpm — are acceptable for the qualitative comparison of condensed models with the full FEM of the rotor. The Campbell diagrams of the frequency lowest ten eigenfrequencies of the test rotor for different level of a rotor condensation ($m_1^{(F)} = m_2^{(F)} = 50; 200$) are shown at Fig. 8.

The relative cumulative error

$$\varepsilon_{50} = \sum_{\nu=2}^{50} \frac{|f_\nu(n, m_1^{(F)}, m_2^{(F)}, \ldots) - f_\nu(n)|}{f_\nu(n)} \tag{30}$$

for $n = 3\,000$ rpm is shown at Fig. 9 in dependence on numbers of master eigenvectors $m_1^{(F)}$ and $m_2^{(F)}$ of the disks.
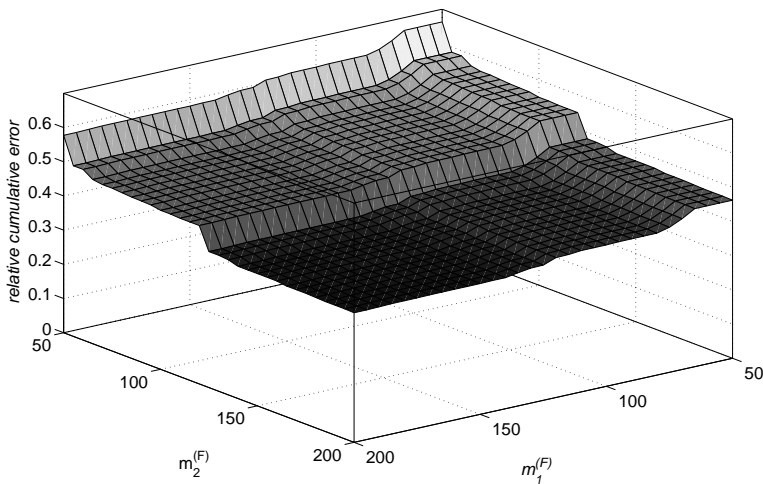

Fig. 9. Relative cumulative error of test rotor eigenfrequencies (for $\nu = 2, 3, \ldots, 50$ and for $n = 3\,000$ rpm).

5. Conclusion

The paper deals with a modelling of rotating shaft vibrations with flexible disks that are ideally fixed to outer shaft surface. The rotating shaft is modelled as a one dimensional continuum on the basis of the Bernoulli-Euler theory. The disks are modelled as a three dimensional continuum discretized using isoparametric hexahedral solid finite elements. The presented approach is based on the modal synthesis method and DOF number reduction corresponding to elastic displacements of the free disk nodes. The displacements of the contact disk nodes on the outer

shaft surface are eliminated by means of shaft nodes displacements. The method allows to introduce continuously distributed centrifugal and gyroscopic effects. The condensed model of the system can be used effectively for modal and sensitivity analysis in state space.

This new approach to rotor vibration modelling was tested for the undamped rotor with two disks supported on rolling-element bearings. The modal values of this test-rotor investigated by using the condensed models were compared with the same values calculated on the full finite element model. From an assesment of the modal assurance of condensed models follows that the developed software in MATLAB code based on the pressented methodology is an effective means for modelling high speed rotor vibrations.

Acknowledgements

References

[1] S. G. Braun, D. J. Ewins, S. S. Rao, Encyklopedia of Vibration, Vol. 1, pp. 256–277, Academic press, San Diego, 2001.

[2] G. Genta, Dynamics of Rotating Systems, Springer Science & Business Media, New York, 2005.

[3] M. Hajžman, J. Šašek, V. Zeman, Vibrations of Rotors with Flexible Disks, Proceedings of conference Engineering Mechanics, Svratka, Institute of Thermomechanics AS CR, 2007, pp. 73–74 (full text on cd-rom).

[4] M. Hajžman, V. Zeman, Noise Analysis and Optimization of Gearboxes, Engineering Mechanics 13 (2) (2006) 117–132.

[5] E. Krǎmer, Dynamics of Rotors and Foundations, Springer-Verlag, Berlin, 1993.

[6] S. S. Rao, The Finite Element Method of Engineering, Pergamon Press, Oxford, 1989.

[7] J. Slavík, V. Stejskal, V. Zeman, Základy dynamiky strojů, Vydavateství ČVUT, Praha, 1997.

[8] J. Šašek, Eigenfrequency Sensitivity analysis of Flexible Rotors, Applied and Computational Mechanics 1 (1) (2007) 289–298.

[9] J. Šašek, Research work to state doctoral examination, University of West Bohemia in Pilsen, Pilsen, 2008.

[10] J. Šašek, V. Zeman, M. Hajžman, Modal properties of rotating disks, Proceedings of 22nd conference Computational Mechanics 2006, Hrad Nečtiny, University of West Bohemia in Pilsen, 2006, pp. 593–600.

[11] T. Yamamoto, Y. Ishida, Linear and Nonlinear Rotordynamics, A Modern Treatment with Applications, John Wiley & Sons, New York, 2001.